15TH IEA HEAT PUMP CONFERENCE
MAY 26–29, 2026 | HOFBURG
VIENNA 2026
DECARBONISATION THROUGH INNOVATION

High temperature heat pumps – An evaluation of the mutual influence between system and control design

Maarten Evens[a,b,*], Alessia Arteconi[a,b]

[a] Department of Mechanical Engineering, KU Leuven, Celestijnenlaan 300, Leuven, 3001, Belgium
[b] EnergyVille, Thor Park 8310, Genk, 3600, Belgium

Abstract

High temperature heat pumps are essential in reaching the decarbonisation targets of the process industry, but there still exist several gaps before widescale application can be reached. One of them relates to increasing the supply temperatures, while achieving acceptable system performances and ensuring system reliability. To this end, combined design and control is key. The goal of this study is to investigate the mutual influence between the system and control design for a water-ammonia prototype applied in the 160 – 200 °C supply temperature range. Hence, this work develops a dynamic simulation model for the prototype and uses the model to evaluate the system's behaviour under varying conditions. A sensitivity analysis on the sizing of the heat exchangers found a stronger sensitivity of the coefficient-of-performance (COP) on sizing the condenser when compared to the evaporator heat exchanger. Moreover, an evaluation on changing the control settings of the compressor, expansion valve and circulation pump at the heat source is performed. Results point out that changing both the control strategy and its control parameters are important key elements to take into account when optimising the design of high temperature heat pumps.

Keywords: High temperature heat pump; Heat exchanger sizing; Control design.

1. Introduction

According to the International Energy Agency (IEA) the industry sector was responsible for emitting 9 Gtons of CO_2 in 2022, representing 25 % of the global energy system emissions [1]. Narrowing down towards the European Union (EU), 66 % of the industrial energy demand was devoted to process heating and was covered for about 78 % by fossil fuels [2]. Therefore, reaching a net-zero emission by 2050 requires thorough decarbonisation of industrial process heat and intensified waste heat recovery. While technologies for supply temperatures below 100 °C are already well proven and commercially available, it is expected that high temperature heat pumps (HTHPs) up to 160 °C [3] will become commercially available by 2026.

Technologies to reach even higher temperature levels than 160 °C are currently under development and Annex 58 on HTHPs expects market entry between 2026 and 2028 [3]. In this context, the UpHeat-INES-2 project [4] aims to achieve supply temperatures in the 160 – 200 °C range with temperature lifts up to 100 °C by using a water-ammonia mixture as a working fluid. As highlighted by Annex 58 on HTHPs [3], the development process for this temperature range is currently focussed on cost optimisation and performance. Also, the review work of Arpagaus et al. [5] suggested future research activities for these temperature levels towards (1) component and system optimisation, (2) cycle efficiency improvement, (3) scale-up towards industrial sizes and (4) environmentally friendly refrigerant development.

With respect to component and system optimisation, Dong et al. [6] investigated the optimal design of a HTHP when applied in a distillation waste heat recovery process. They proposed a bi-level programming model to optimise the design of the HTHP system when being subject to multiple operating conditions and

* Corresponding author.
E-mail address: maarten.evens@kuleuven.be

15th IEA Heat Pump Conference 2026 - HTH2.2 - https://doi.org/10.23697/cjcm-6y80

objectives. They found a reduction of 17.5 % in average carbon emissions when compared to conventional design methodologies. Regarding the heat exchangers, Wu et al. [7] assessed the potential design impact of selecting different two-phase heat transfer correlations in HTHPs. They found that the design of the condenser heat exchanger was more impacted than the evaporator heat exchanger and also revealed that the dimensions, costs and carbon emissions were significantly affected by the selected correlation. In fact, the coefficient-of-performance (COP) varied by 0.38 % under design conditions, but by 3.27 % under off-design conditions for the inlet temperature from the heat source. Given the requirement for reaching high temperature levels with HTHPs, several works also focussed on reducing the compressor discharge temperature [8]. For instance, Sadeghi et al. [9] investigated the potential of using a district heating network as a heat source to deliver 1 MW of process heat at 160 °C. A cascade system with butane in the low-temperature loop and steam in the high-temperature loop was proposed and where a water injection loop was used to limit the compressor discharge temperature.

In addition to a proper design, the control of the actual HTHP system is also a crucial aspect when integrating the HTHP system in fluctuating industrial processes. To this end, a stable operating point for the compressor(s), expansion valve(s) and auxiliary equipment such as circulation pumps has to be found. To this end, Liu et al. [10] used a multi-variable extremum seeking control strategy on a HTHP with two injection loops and stated that many studies focus on optimising the number and location of injection ports rather than evaluating the interplay and relationships between injection ports under variable conditions. In addition, Gong et al. [11] improved the COP by 7.7 % by using an extremum seeking control on the vapor injection loop for a 200 kW HTHP. Al-Badri al. [12] also showed the importance of investigating potential cross-couplings in the HP control logics to ensure stability and to avoid interaction between control variables. Finally, Wang et al. [13] showed that by optimising the settings of a proportional-integral-derivative (PID) controller through a fuzzy strategy the average heat transfer coefficient on a single-tube heat exchange platform could be increased.

From the existing literature, it can be concluded that optimising the performance of an overall HP system requires a combinatory approach in which both the component design and control design are simultaneously investigated. Therefore, a combined design and control of the overall system is required to further reduce the costs and increase the adoption of HTHPs in the industry. As a first step towards integrated design of HTHPs, this work aims to investigate the mutual influence between design and control on the HTHP prototype of the UpHeat-INES project [4]. Through this investigation, obtaining proper control settings to run the first experiments on the prototype will also become feasible. To reach these objectives, a dynamic model in the Modelica language was developed and tested for different sizes of the heat exchangers along with different controller settings on the compressor, expansion valve and circulation pump connected to the heat source. The performance will be evaluated in both steady-state and dynamic conditions to take into account the variability in operating conditions.

This paper will be structured as follows. Section 2 presents the methodological approach, including the dynamic model and load profiles. Section 3 firstly elaborates on the effects of sizing the heat exchangers, followed by an evaluation of the control settings for the compressor, expansion valve and circulation pump. Finally, the conclusion summarises the main outcomes of this work and defines future research directions.

2. Methods

This section starts with briefly describing the HTHP prototype of the UpHeat-INES project [4], followed by the dynamic simulation model. Furthermore, a definition and reasoning on the adopted load profiles to assess the performance and controllability of the HTHP system is presented

2.1. Prototype and model description

The model used for the purpose of this work is based on the HTHP prototype from the UpHeat-INES project [4]. The project aims to develop a water-ammonia HTHP prototype for process heat temperatures in the 160 – 200 °C range and uses an oil-free twin-screw compressor with refrigerant injection. Figure 1 shows a simplified hydraulic overview of the HTHP system, including an indication of its main components and was modelled in Modelica using TIL-Suite from TLK [14]. Given that the prototype will be exploited with pure water as a refrigerant during the initial phase of the project, the model also uses pure water. The heat source and heat sink use thermal oil from the Therminol66 type and have nominal flow rates of 1.691 kg/s for the heat source and 1.4 kg/s for the heat sink.

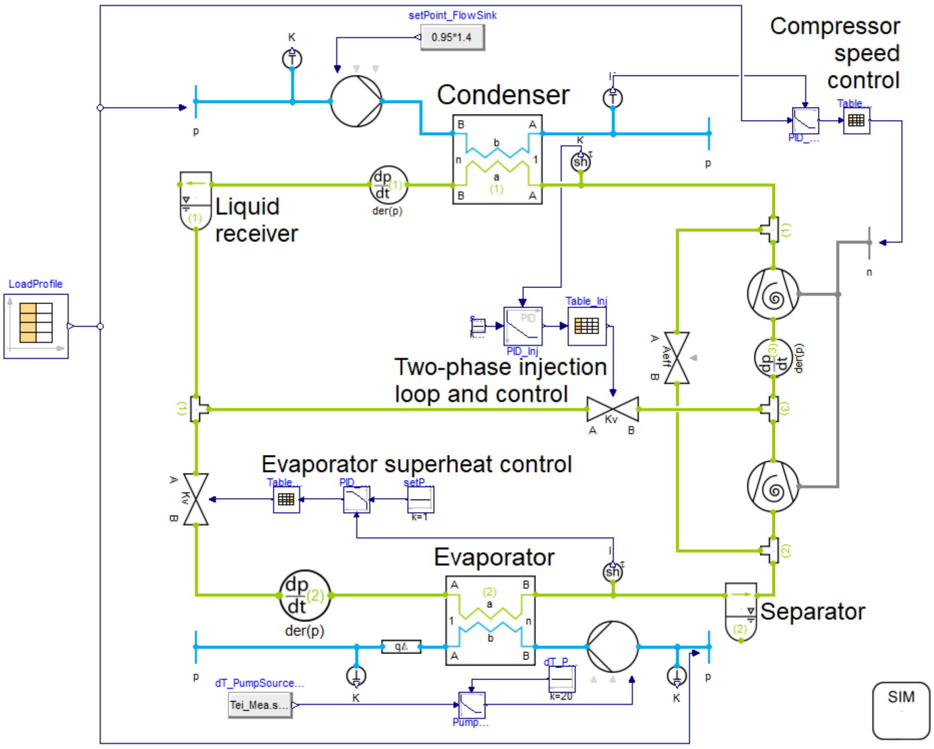

Figure 1. Overview of high temperature heat pump dynamic simulation model. Green lines: refrigerant circuit. Light blue lines: thermal oil circuits. Dark blue lines: control signals.

Concerning the heat exchanger parameterisation, Table 1 provides a summary of the main characteristics. Technical manufacturer specifications were used whenever available. A simplification was required for the condenser heat exchanger as the real prototype uses a shell and plate heat exchanger, but this type of heat exchanger was not available in the TIL library and therefore represented with a plate heat exchanger instead. Moreover, given the aim to analyse both steady-state and dynamic operation, preference was given to using correlations for the heat transfer coefficients and the closest fitting correlations were selected.

Table 1. Characteristics of the modelled heat exchangers.

Key characteristic	Component: evaporator heat exchanger	Component: condenser heat exchanger
Number of plates	110	165
Heat exchanger type	Plate and modelled as plate	Shell and plate modelled as plate
Plate length x width (m x m)	0.439 x 0.179	0.439 x 0.179
Plate material	Stainless steel	Stainless steel
Discretisation along flow path	15 elements	15 elements
Refrigerant pressure drop	Neglected: 0 Pa	Neglected: 0 Pa
Thermal oil pressure drop	5290 Pa at 1.691 kg/s	Neglected: 0 Pa
Refrigerant heat transfer	Correlations according to Steiner for evaporation and Gnielinski-Dittus-Boelter for single phase	Correlations according to Shah for condensation and Gnielinski-Dittus-Boelter for single phase

In agreement with the prototype, a 1 K superheat setpoint at the exit of the evaporator heat exchanger is used. A 1 l separator after the evaporator heat exchanger was used for numerical stability in the model and could be justified by taking into account that piping volumes are neglected in the simulation model.

Regarding the compression process, the oil-free compressor has four inlet connections, i.e. (1) the main inlet coming from the evaporator heat exchanger, (2) a low-pressure bearing lubrication connection close to the suction port, (3) a high-pressure bearing lubrication connection close to the discharge port and (4) a two-phase injection connection allowing to reduce the compressor discharge temperature. Due to the non-availability of experimental data, the current work solely incorporates the two-phase injection loop which is aimed to limit the discharge temperature of the compressor. In fact, the envisioned control in the prototype for the first experimental tests is to limit the superheating at the discharge port of the compressor at 40 K. To incorporate the two-phase injection loop, the twin-screw compressor is discretised into two compressor elements with an equal built-in volume ratio (BVR) as outlined in Eq. (1) and where the two-phase injection loop is connected between the two compressor elements.

$$BVR_{single} = \sqrt{BVR_{tot}} \tag{1}$$

Herein, BVR_{tot} and BVR_{single} hold the BVR of the total compressor and the BVR of a single compressor element, respectively. The displacement volume $V_{displ,2}$ for the second compressor element can be retrieved through Eq. (2) by taking into account the BVR and displacement volume of the first compressor element. Both compressor elements have identical rotational speeds.

$$V_{displ,2} = \frac{V_{displ,1}}{BVR_{single}} \tag{2}$$

As a starting point on the control logics, three proportional-integral-derivative (PID) controllers were used and manually tuned to reach control stability. The first PID controller regulates the compressor speed to control the oil supply temperature towards the load. A second PID controller regulates the main expansion valve to control the superheat at the outlet of the evaporator heat exchanger, while a third PID controller is aimed to keep a 40 K superheat at the discharge port of the compressor.

2.2. Case study description

In light of evaluating the influence between system design and control, the investigation is separated into two steps, i.e. (1) component design with a specific focus on heat exchanger sizing and (2) control design.

2.2.1. Step 1: steady-state load profiles to evaluate impact of heat exchanger sizing

Figure 2 shows the adopted load profile to evaluate the impact of selecting a different size for the heat exchangers. Independent variations of ± 10 %, ± 20 % and ± 40 % on the number of plates were evaluated for both the evaporator and condenser heat exchanger, eventually leading to 49 unique designs. The load profile exhibits a total of 27 different operating conditions to take into account the potential variability in operating conditions in industrial environments, while sufficient time is given to reach steady-state conditions for a proper analysis. To solely limit the analysis on heat exchanger sizing, a minimum and maximum compressor speed constraint was not implemented, ensuring that the requested load is always fulfilled. Similar, but milder conclusions were also found when setting speed constraints.

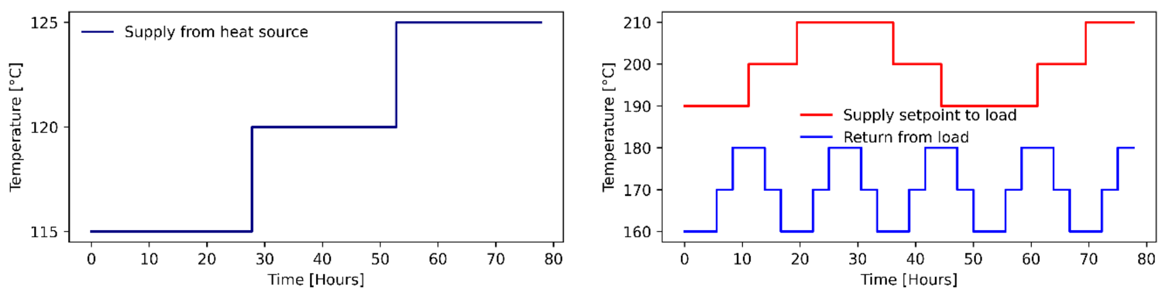

Figure 2. Steady-state load profiles to evaluate the impact of heat exchanger sizing.

2.2.2. Step 2: dynamic load profiles to evaluate impact of controller settings

Figure 3 presents the dynamic load profile used to investigate the impact of setting different controller parameters and/or control logics. The profile exhibits less extreme inlet and outlet temperature conditions at the load side when compared to the load profiles used for the steady-state performance evaluation. This choice was based on the preceding steady-state performance analysis where the HTHP system was occasionally operating outside the envisioned working range for the HTHP prototype. While being helpful to evaluate the sizing impact of the heat exchangers, operating outside the working range is hard to justify when one wants to determine the initial control parameters for the prototype. In addition to setting less extreme load conditions, the duration of each condition is also shortened to such an extent that the HTHP system is near steady-state before initiating the next condition. Such an approach enables an easier evaluation of the dynamic operation and impact of having different controller settings. Given the aim to find the start values for the prototype controller parameters, limitations on the compressor speed were also implemented and set close to the working envelope of the compressor drive, i.e. from 30 Hz until 158 Hz. The load flow rate remained constant at 95 % of the nominal flow rate of 1.4 kg/s.

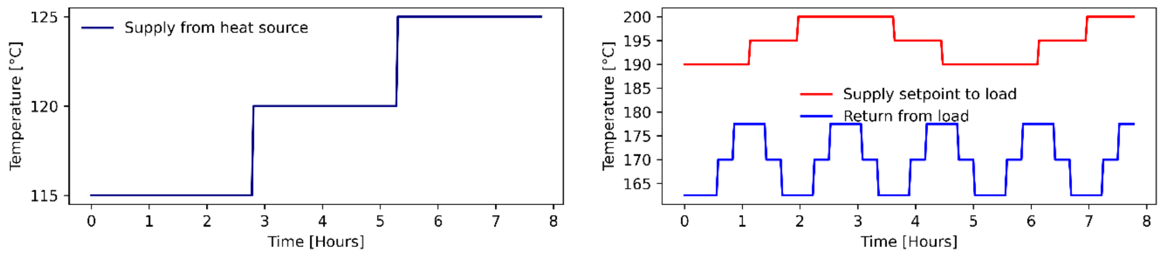

Figure 3. Dynamic load profiles to evaluate the impact of controller settings.

A sensitivity analysis is performed on the control parameters for the compressor and expansion valve in the main refrigerant circuit. The range for each control parameter is composed by evaluating if further increasing or decreasing still leads to stable operation.

Concerning the main expansion valve controller which is comparing the actual superheat at the outlet of the evaporator heat exchanger to its setpoint value, the ranges were:

- [0.2 – 10] for the proportional gain with a total of eight different values
- [5 s – 105 s] for the integral time with a total of four different values
- [0.0001 s – 0.5 s] for the derivative time with a total of two different values. A derivative time of 0.0001 s led to instability issues when sudden changes in the heat source conditions occurred. For the remainder of this work, the derivative time of the main expansion valve controller was therefore fixed at 0.5 s and could not be further reduced to prevent oscillations related to too quick control actions.

For the compressor speed controller which compares the actual supply temperature of the thermal oil to the load to its setpoint value, the considered ranges were:

- [0.5 – 4] for the proportional gain with a total of seven different values
- [15 s – 500 s] for the integral time with a total of nine different values
- [0.001 s – 1 s] for the derivative time with a total of two different values. Contrarily to the main expansion valve controller, opting for a relatively high derivative time for the compressor speed controller led to instability issues, potentially caused by the time delay between the control action taken on the compressor speed and the visible effect at the heat transfer in the condenser heat exchanger. For the remainder of this work, the derivative time of the compressor speed controller was therefore fixed at 0.001, eventually leading to a negligible impact from the derivative control action.

In addition to investigating the impact of having different PID controller settings for the compressor and main expansion valve, three different control strategies for the circulation pump at the heat source were investigated. To this end, the pressure drops related to the evaporator heat exchanger and laboratory equipment connected to the prototype were modelled to well assess the potential impact on the electricity consumption of the circulation pump. The investigated control strategies were:

- Constant flow rate at an identical flow percentage as the flow rate at the heat sink, i.e. if the pump at the heat sink runs at 100 %, the heat source pump also runs at 100 %. For simplicity reasons, the requested flow rate by the load is considered constant and therefore also the heat sink flow rate is considered constant.
- Variable flow rate as a function of the compressor speed as determined in Eq. (3).

$$minimum\left(\dot{m}_{source,max}\,;\dot{m}_{source,max}\cdot\left(\frac{1}{3}+\frac{2}{3}\cdot\left(\frac{f_{comp}-f_{comp,min}}{f_{comp,max}-f_{comp,min}}\right)\right)\right) \tag{3}$$

Within Eq. (3), f_{comp}, $f_{comp,min}$ and $f_{comp,max}$ denote the actual, minimum and maximum compressor frequency. It is assumed that the pump can regulate its speed between 33 % and 100 %. $\dot{m}_{source,max}$ is the maximum achievable flow rate with the pump running at its nominal speed.

- Variable flow rate to keep a constant temperature difference between the thermal oil inlet and outlet of the evaporator heat exchanger. Four different temperature difference setpoints are investigated, i.e. 10 K, 20 K, 30 K and 40 K. Similar to the previous approach, a pump speed control range between 33 % and 100 % is used.

3. Results

3.1. Step 1: steady-state performance evaluation

Figure 4 overviews the impact on the average electrical power of the HTHP when sizing differently the heat exchangers. The average electrical power over all 27 different operating conditions from the load profile in Figure 2 is plotted and a logarithmic trendline was fitted. Furthermore, Figure 5 shows the impact on the average discharge temperature and compressor speed. Interpreting these figures, it is found that oversizing both heat exchangers leads to efficiency gains due to reducing the pressure difference that has to be overcome by the compressor as the heat transfer between the thermal oil and refrigerant improves with increasing heat exchange areas. However, the impact of oversizing the condenser is greater than the evaporator which is also visible in Figure 4 with higher slopes for changing the condenser size than when changing the evaporator size. From an economical point of view, the found trend and difference between both heat exchangers indicates that if the cost for oversizing the evaporator and condenser heat exchanger is comparable, oversizing the condenser should receive higher priority as the impact on the overall system's efficiency is larger.

While the positive impact of oversizing the heat exchangers on the electrical power was rather expected, this was not the case for the impact on the compressor speed. The results indicate that oversizing the evaporator/condenser leads to a decrease/increase in the compressor speed, respectively. Especially, the increasing compressor speed for a larger condenser size requires further analysis. Assuming steady-state conditions in which the load is met, obtaining a lower electrical power due to condenser oversizing inherently requires a larger evaporator power. To this end, a slightly lower evaporating pressure when oversizing the condenser heat exchanger is required and is also visible in the systems's behaviour. The decrease in the evaporating pressure is however smaller than the decrease in the condensing pressure and explains why the electrical power decreases. Given the lower pressure difference to be overcome by the compressor, the superheat at the compressor's discharge port also reduces as evidenced by the average discharge temperature of the second compressor element as shown in Figure 5. Taking into account the two-phase injection circuit being controlled to maintain a superheat setpoint of 40 K at the compressor's discharge port, the required mass flow rate from this particular loop can thus also be reduced. Therefore, the refrigerant flow passing through the evaporator heat exchanger should increase in order to cover the thermal load and to reach this higher refrigerant flow rate, a higher compressor speed is needed.

The impact of this finding with the current control design of the two-phase injection loop has also a downside when one would include minimum and maximum speed constraints on the compressor as used in the prototype. In those cases, oversizing the condenser leads to faster reaching the maximum speed of the compressor if the superheat setpoint of the two-phase injection loop would not be changed. Given that the compressor has to overcome a reduced pressure difference which leads to a lower discharge temperature, controlling the two-phase injection loop with a different superheat setpoint at the discharge port of the compressor could potentially lead to a reduction in the compressor speed. However, experiments on the actual prototype for such a control strategy are needed to fully take into account the bearings loop in order to properly retrieve the remaining control potential for the two-phase injection loop and will be part of a future work.

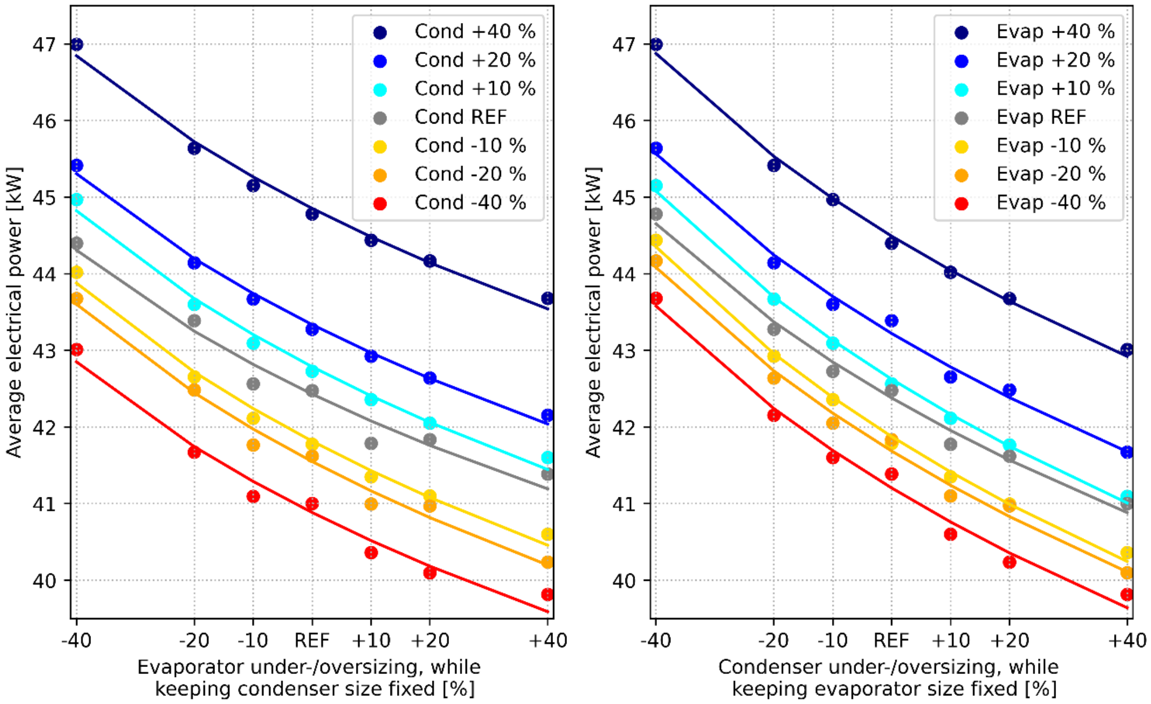

Figure 4. Result overview of steady-state performance evaluation in which the size of one heat exchanger was varied while keeping the other fixed at a certain size. The figure legend indicates the sizing of the heat exchanger that remains fixed. Left: Variation of the average electricity consumption when changing the evaporator size for a certain fixed condenser size. Right: Variation of the average electricity consumption when changing the condenser size for a certain fixed evaporator size. REF refers to the reference condition according to the prototype design as reported in Table 1.

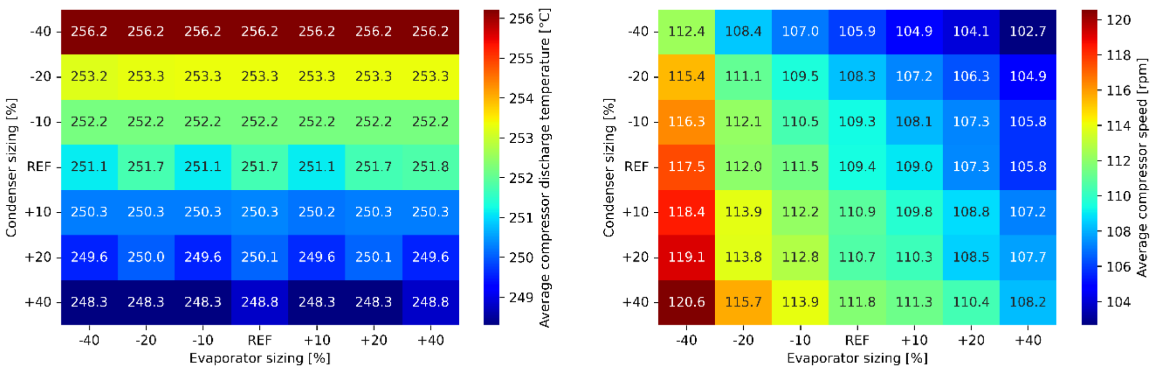

Figure 5. Heat map result overview of steady-state performance evaluation. Left: average compressor discharge temperature. Right: average compressor speed.

3.2. Step 2: dynamic performance under different control settings and strategies

3.2.1. Effect of changing the main expansion valve control settings

As already listed in the methodological approach, setting a derivative time of 0.5 s was required to prevent oscillations as a quick response of the expansion valve can be needed, especially in case of changing conditions at the heat source. Further increasing the derivative time occasionally led to too quick control responses and unnecessary system oscillations and was therefore not further evaluated. Regarding the integral time, setting integral times above 105 s led to too slow responses of the expansion valve with the risk of having two-phase conditions at the outlet of the evaporator heat exchanger.

Taking into account these limitations on the integral time and derivative time, Figure 6 summarises the remaining cases. The impact on the total electricity consumption and cumulative control error on the superheat according to Eq. (4) was further assessed. The purpose of Eq. (4) is to evaluate how quick the controller can bring the superheat close to its setpoint value. In the right part of Figure 6 the noticed behaviour from the simulations were grouped into nine different classes with further explanation in Table 2. Using a proportional gain of 0.61 with an integral time of 5 s and a derivative time of 0.5 s provided the best trade-off between taking quick, fast enough responses in order to limit the deviation from the superheat setpoint, while ensuring stability by preventing an oscillating behaviour of the expansion valve. From the performance metrics in Figure 6, the impact on the electricity consumption for different controller settings on the expansion valve remains limited, while larger effects can be seen on the accumulated error on the superheat over time ($SH_{err,cum}$) as determined by Eq. (4). Therefore, those control settings that minimise $SH_{err,cum}$ without reaching oscillations should be selected.

$$SH_{err,cum} = \sum_{t=1}^{N} \left| superheat_{evaporator,setpoint,t} - superheat_{evaporator,measured,t} \right| \quad (4)$$

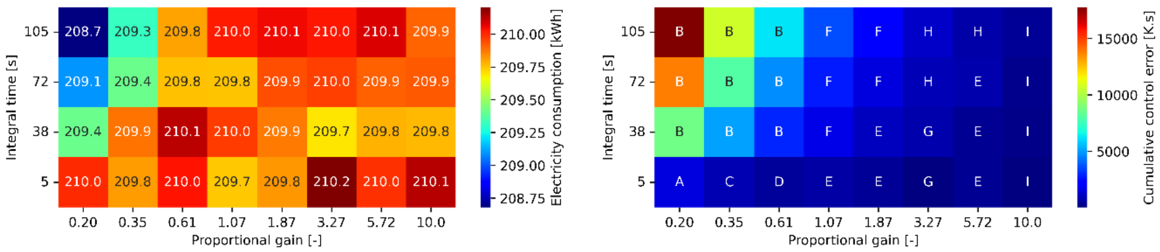

Figure 6. Heat map result overview of dynamic performance evaluation by evaluating different parameter settings for the main expansion valve controller. Left: total electricity consumption over entire simulation. Right: cumulative control error on the superheat at outlet of evaporator heat exchanger as determined by Eq. (4) and where each control parameter combination is classified into a feasibility class from class A until class I with further explanation in Table 2.

Table 2. Description of feasibility classes to evaluate the PID control parameters of the main expansion valve.

Class	Feasibility discussion
A	Feasible, but relatively large overshoot due to low integral time and low proportional gain
B	Unfeasible, too slow response due to low proportional gain and high integral time
C	Feasible, but relatively large overshoot due to low integral time
D	Feasible with sufficiently quick control responses, while preventing oscillations
E	Unfeasible, oscillations due to increased proportional gain and low integral time
F	Feasible, but large overshoot due to increased proportional gain
G	Feasible, but small oscillations visible due to large proportional gain with low integral time
H	Feasible, but large overshoot due to high proportional gain and slow control due to high integral time
I	Unfeasible, too sensitive responses due to large proportional gain

3.2.2. Effect of changing the compressor control settings

After setting the PID control parameters for the main expansion valve, the sensitivity analysis on the PID parameters for the compressor speed control was performed. Concerning the derivative time, setting a high derivative time for the compressor speed controller led to instability issues, potentially linked to the time delay between taking a control action on the compressor speed and the measuring the actual change in the supply temperature of the thermal oil circuit towards the load. Therefore, the derivative time of the compressor speed controller was fixed at 0.001 which is close to switching of the derivative control action.

Figure 7 shows the metrics used to evaluate the performance of the different control settings. Given that the compressor speed is regulated to control the supply temperature towards the load, the accumulated temperature error over time $T_{c,o,err,cum}$ according to Eq. (5) is used. Similar to the evaluation on the expansion valve, the results in Figure 7 are categorised into several classes with further clarification of these classes in Table 3.

Comparing the sensitivity of the electricity consumption on changing the PID control parameters, a greater influence is found on changing the compressor control settings than changing the main expansion valve control settings. Indeed, the difference between the minimum and maximum electricity consumption mentioned in Figure 6 and Figure 7 is only 0.73 % for the expansion valve controller and already 1.20 % for the compressor speed controller. Therefore, it is concluded that finding the right set of parameters for the compressor speed controller should receive a higher priority than for the expansion valve controller. The adopted setting for the HTHP prototype with a proportional gain of 2, integral time of 60 s and derivative time of 0.001 s was selected as a compromise between operational stability without oscillating behaviour and quick control responses in which the accumulated temperature error ($T_{c,o,err,cum}$) from Eq. (5) remains low.

$$T_{c,o,err,cum} = \sum_{t=1}^{N} \left| T_{condenser,outlet,oil,setpoint,t} - T_{condenser,outlet,oil,measured,t} \right| \tag{5}$$

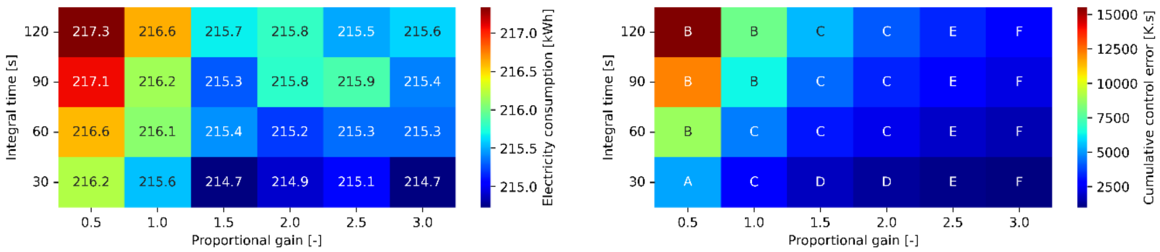

Figure 7. Heat map result overview of dynamic performance evaluation by evaluating different parameter settings for the compressor speed controller. Left: total electricity consumption over entire simulation. Right: cumulative control error on the supply temperature to the load as determined by Eq. (5) and where each control parameter combination is classified into a feasibility class from class A until class F with further explanation in Table 3.

Table 3. Description of feasibility classes to evaluate the PID control parameters of the compressor.

Class	Feasibility discussion
A	Unfeasible due to low integral time which lead to unrealistic ramping rates
B	Feasible, but slow response due to low proportional gain and relatively high integral time
C	Feasible with sufficiently quick control responses, while preventing oscillations
D	Unfeasible, high proportional gain with low integral time reaching unrealistic ramping rates
E	Feasible, but at the limit of stability due to the large proportional gain
F	Unfeasible, too sensitive responses with oscillations due to large proportional gain

3.2.3. Effect of setting a different control strategy on the circulation pump of the heat source

Having found the PID control parameters for the compressor and main expansion valve, an evaluation on the impact of setting a different control strategy on the heat source was evaluated. Table 4 summarises the performance evaluation when using different control strategies on the circulation pump at the heat source. Given that the first case with a constant pump speed is close to the maximum speed, it is concluded that this option is the preferred option from an energy point of view. With such a control strategy, the evaporating pressure is maximised, leading to a lower pressure difference to be overcome by the compressor and ultimately to a lower electricity consumption of the compressor. Between all the different cases, a maximum difference of 0.57 bar in the evaporating pressure could be seen. Solely the case with a pump control aiming to achieve a 10 K temperature difference between the thermal oil inlet and outlet shows a slightly lower electricity consumption as the pump is generally running at its absolute maximum speed. Given that the pump consumption is of a different magnitude than the compressor consumption, it is recommended to focus on minimising the compressor consumption.

Keeping the flow rate from the heat source continuously constant has the downside of reaching a less responsive system towards changing boundary conditions as evidenced by the accumulated errors over time ($SH_{err,cum}$ and $T_{c,o,err,cum}$), shown in Table 4. In fact, with a constant flow rate from the heat source, solely the expansion valve can be used to regulate the evaporator capacity. In light of this, changing the heat source flow rate could support in finding a quicker system balance by also becoming able to regulate the evaporator's capacity. From the evaluated cases that aim to maintain a constant temperature difference between the thermal oil inlet and outlet, the case with a 20 K temperature difference was found as the strategy that leads to covering the entire working range of the circulation pump. Contrarily, the 10 K strategy led to running at the absolute maximum pump speed, while the 40 K strategy was mainly running at the minimum pump speed. As evidenced by Figure 8, the 20 K temperature difference strategy and the control strategy directly proportional to the compressor speed also have very similar control responses and flow rates, but with slightly quicker control responses for the 20 K strategy. With a focus on both electricity consumption and controllability of the entire heat pump system, the 20 K temperature difference control strategy could be recommended.

Moreover, the control interference between the pump control and compressor control should be well investigated to avoid oscillations. In fact, increasing the pump speed increases the evaporating pressure, which should also lead to less compressor work, which could then lead to a lower compressor speed. Given the lower compressor speed, the extracted power from the evaporator is also affected and also changes the oil return temperature at the heat source, which then again leads to a change in the pump speed. Therefore, a proper tuning and dynamic analysis of the PID controls is required to prevent introducing oscillations in the system and directly relating the pump control strategy to the compressor speed should be avoided.

Table 4. Result overview of setting different control strategies and control parameters for the heat source circulation pump.

Heat source pump control strategy	Electricity consumption compressor (kWh)	Electricity consumption pump heat source (kWh)	$SH_{err,cum}$ (K.s)	$T_{c,o,err,cum}$ (K.s)
Constant flow	209.318	5.608	508	2330
Function of compressor speed	225.752	2.207	516	2181
Temperature difference of 10 K	207.083	6.097	527	2257
Temperature difference of 20 K	226.809	2.257	548	2098
Temperature difference of 30 K	256.544	0.477	398	14919
Temperature difference of 40 K	260.219	0.241	254	39295

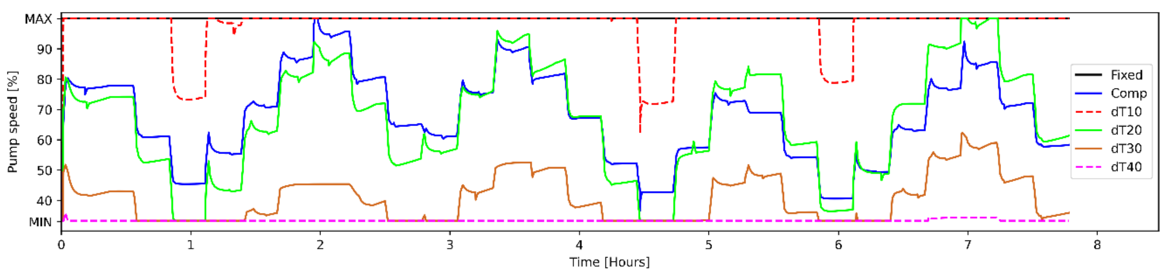

Figure 8. Percentual pump speeds under different control strategies on the circulation pump at the heat source. Fixed refers to setting a constant fixed speed and Comp directly relates the pump speed to the compressor speed via Eq. (3). dT10, dT20, dT30 and dT40 aim to keep a constant temperature difference between the supply and return oil from the heat source of 10 K, 20 K, 30 K and 40 K, respectively.

4. Conclusion

This work evaluates the influence of the component and control system design on a high temperature heat pump. Regarding the component design, the effect of changing the heat exchanger sizes is investigated by varying the number of plates within ± 40 % from the design conditions. It is found that changing the size of the condenser heat exchanger has a stronger effect as the gain in the COP is larger than the gain in the COP for the same oversizing rate of the evaporator. Given the presence of intercooling and bearing loops, the effect of these loops was also investigated. However, the results show that detailed experiments to fully take into account the influence from both loops are required to properly assess the potential contribution for each of these individual loops. A second part of this work investigates the influence of control settings and strategies on the expansion valve, compressor and circulation pump at the heat source and determines the initial control settings for the experimental tests on the actual prototype. Results indicate the necessity to tune the control parameters to reach quick system responses, while avoiding system oscillations. The effect on the energy consumption remains limited. However, the compressor speed control showed a stronger influence on the energy consumption when compared to the expansion valve control. Regarding the pump control strategies, maintaining a constant temperature difference of 20 K between the thermal oil inlet and outlet at the heat source led to a trade-off between quick control responses and increased energy consumption. Future work on the prototype will allow to validate the dynamic simulation model and to investigate more advanced control strategies such as gain scheduling or even model predictive control.

Acknowledgements

We gratefully acknowledge the financial support of the Flemish Government and Flanders Innovation Entrepreneurship (VLAIO) through the Moonshot project Upheat-INES-2 (HBC.2022.0539 – UPHEAT-INES-2: Upgraded high temperature heat in energy intensive sectors 2.0).

References

[1] International Energy Agency (IEA), "Energy system: industry." [Online]. Available: https://www.iea.org/energy-system/industry

[2] R. de Boer *et al.*, "Strengthening Industrial Heat Pump Innovation: Decarbonizing Industrial Heat," 2020.

[3] B. Zühlsdorf, *IEA: Annex 58 about HTHP, Task 1: Technologies – State of the art and ongoing developments for systems and components*. Danish Technological Institute (DTI), 2023. [Online]. Available: https://heatpumpingtechnologies.org

[4] Catalisti, "UpHeat-INES-2." [Online]. Available: https://www.moonshotflanders.be/en/projects/upheat-ines-2

[5] C. Arpagaus, F. Bless, M. Uhlmann, J. Schiffmann, and S. S. Bertsch, "High temperature heat pumps: Market overview, state of the art, research status, refrigerants, and application potentials," *Energy*, vol. 152, pp. 985–1010, 2018, doi: 10.1016/j.energy.2018.03.166.

[6] S. Dong, P. Hu, C. Zhang, X. Hu, W. Zhuang, and D. Wu, "How to optimally design industrial high-temperature heat pump for multiple objectives and working conditions?," *Energy*, vol. 329, no. March, p. 136830, 2025, doi: 10.1016/j.energy.2025.136830.

[7] D. Wu *et al.*, "Heat exchanger design and performance evaluation for a high-temperature heat pump system under different two-phase correlations: 4E analysis," *Appl. Energy*, vol. 384, no. January, 2025, doi: 10.1016/j.apenergy.2025.125492.

[8] R. Wang, H. Yan, D. Wu, J. Jiang, and Y. Dong, "High temperature heat pumps for industrial heating processes using water as refrigerant," *Energy*, vol. 313, no. May, 2024, doi: 10.1016/j.energy.2024.133847.

[9] M. Sadeghi, T. Petersen, Z. Yang, B. Zühlsdorf, and K. S. Madsen, "Thermal design and optimization of high-temperature heat pump integrated with district heating benchmarked in Denmark for process heat supply," *Int. J. Refrig.*, vol. 159, no. December 2023, pp. 356–370, 2024, doi: 10.1016/j.ijrefrig.2023.12.025.

[10] G. Liu, Z. Lu, Y. Yao, and Y. Gong, "Multi-variable extremum seeking control for high temperature heat pump system incorporating double refrigerant injection," *Int. J. Refrig.*, vol. 152, no. March, pp. 1–15, 2023, doi: 10.1016/j.ijrefrig.2023.04.010.

[11] Y. Gong, G. Liu, and Z. Lu, "Extremum seeking control for real-time optimization of high temperature heat pump systems incorporating vapor injection," *Therm. Sci. Eng. Prog.*, vol. 42, no. April, p. 101867, 2023, doi: 10.1016/j.tsep.2023.101867.

[12] A. R. Al-Badri and A. H. Al-Hassani, "A control method using adaptive setting of electronic expansion valve for water chiller systems equipped with variable speed compressors," *Int. J. Refrig.*, vol. 119, pp. 102–109, 2020, doi: 10.1016/j.ijrefrig.2020.06.008.

[13] J. F. Wang *et al.*, "Performance analysis and PID control strategy optimization of the electronic expansion valve on the single-tube heat exchange experimental platform," *Appl. Therm. Eng.*, vol. 250, no. April, 2024, doi: 10.1016/j.applthermaleng.2024.123532.

[14] TLK Energy, "TIL Suite," 2024, 3.16.0. [Online]. Available: https://tlk-energy.de/en/software/til-suite